Electronic Supplementary Information for:

Solution-Processed Small Molecules Based on Benzodithiophene and Difluorobenzothiadiazole for Inverted Organic Solar Cells

Xunfan Liao[a], Feiyan Wu[a], Lie Chen*[a,b], Yiwang Chen[a,b]

[a]College of Chemistry/Institute of Polymers, Nanchang University, 999 Xuefu Avenue, Nanchang 330031, China

[b]Jiangxi Provincial Key Laboratory of New Energy Chemistry, Nanchang University, 999 Xuefu Avenue, Nanchang 330031, China

*Corresponding author. Tel.: +86 791 83968703; fax: +86 791 83968830. E-mail: chenlie@ncu.edu.cn (L. Chen).

Xunfan Liao and Feiyan Wu contributed equally to this work.

1. Materials

All reactions and manipulations were operated under argon atmosphere and all the starting materials were purchased from commercial suppliers and used without further purification. Chloroform, Ag (99.999%), MoO_3 (99.999%), $PC_{61}BM$ (99.9%), $PC_{71}BM$ (99.9%) and other materials were purchased from Alfa, or Aldrich and without further purification. Indium-tin oxide (ITO) glass was purchased from Delta Technologies Limited, whereas PEDOT:PSS (Baytron PAl4083) was obtained from Bayer Inc. 4,7-Bis(5-bromothiophene-2-yl)-5,6-difluorobenzo[c][1,2,5]thiadiazole (compound 2) and 4,7-bis(2-bromo-5-thien)-2,1,3-benzothiadiazole (compound 3) were purchased from Derthon. Tetrakis(triphenylphosphine)palladium(0) [$Pd(PPh_3)_4$] was obtained from Energy Chemical.

2. Experimental

The ^1H and ^{13}C NMR spectra were recorded in deuterated solvents on a Bruker ADVANCE 400 NMR Spectrometer. 1H NMR chemical shifts were reported in ppm downfield from tetramethylsilane (TMS) reference using the residual protonated solvent as an internal standard. Thermogravimetric analysis (TGA) was carried out on a PerkinElmer TGA 7 instrument for thermal analysis at a heating rate of 10 °C/min under nitrogen. UV-vis absorption spectra were recorded on a Perkin Elmer Lambda 750 spectrophotometer. Cyclic voltammetry (CV) was performed a Zahner IM6e electrochemical workstation. X-ray diffraction (XRD) was performed on a Bruker D8 Focus X-ray diffractometer operating at 30 kV and 20 mA with a copper target (λ= 1.54 Å) and at a scanning rate of 1°/min. Atomic force microscopic (AFM) images were carried on a Nanoscope III A (Digital Instruments) scanning probe microscope using the tapping mode. The specimen for AFM measurement was prepared as same as the devices fabrication other than without MoO_3/Ag was vacuum evaporated on the active layer. Transmission electron microscopy (TEM) images were performed on a JEOL-2100F transmission electron microscope and an internal charge-coupled device (CCD) camera. The specimen for TEM measurement was prepared by spin casting the blend solution on ITO/PEDOT:PSS substrate, then floating the film on a water surface, and transferring to TEM grids.

Space-charge-limited-current (SCLC) mobility measurement. The hole-only devices used a diode configuration of ITO/PEDOT:PSS/active layer/MoO_3/Ag by taking current-voltage curve in the range of 0-6 V. The carrier mobilities were measured using the SCLC model, which is described by $J = 9\varepsilon_0\varepsilon_r uV^2/8L^3$, where J is the current density, L is the film thickness of active layer, ε_0 is the permittivity of free space (8.85×10^{-12} F m^{-1}), ε_r is the relative dielectric constant of the transport medium, *u* is the hole or electron mobility, *V* is the internal voltage in the device and $V = V_{appl}-V_r-V_{bi}$, where V_{appl} is the applied voltage to the device, V_r is the voltage drop due to contact resistance and series resistance across the electrodes, and V_{bi} is the built-in voltage due to the relative work function difference of the two electrodes.[1-3] The thickness of the BHJ blend for SCLC measurement was about 110 nm. The hole-mobility can be calculated from the slope of the $J^{1/2}$~V curves.

3. Supporting Figures and Tables

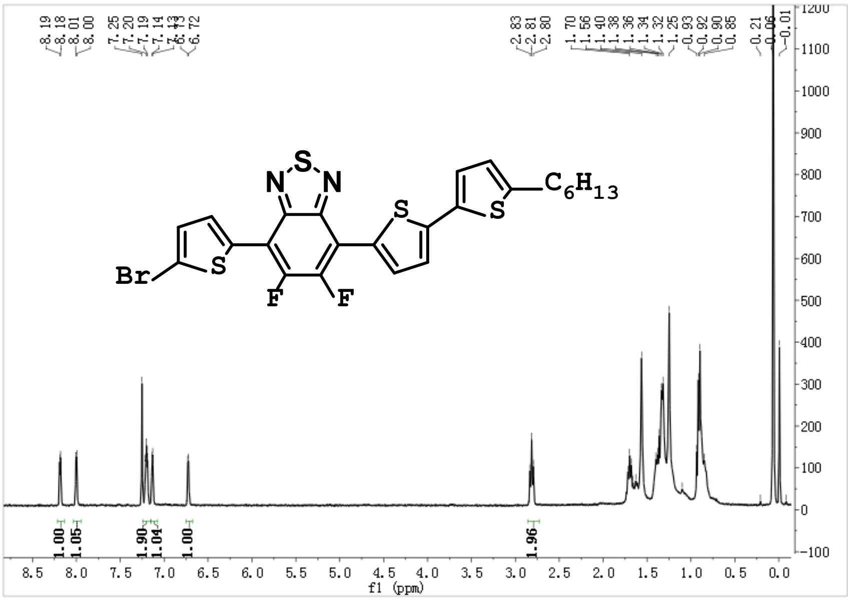

Figure S1. ^{1}H NMR spectra of compound **4** in $CDCl_3$.

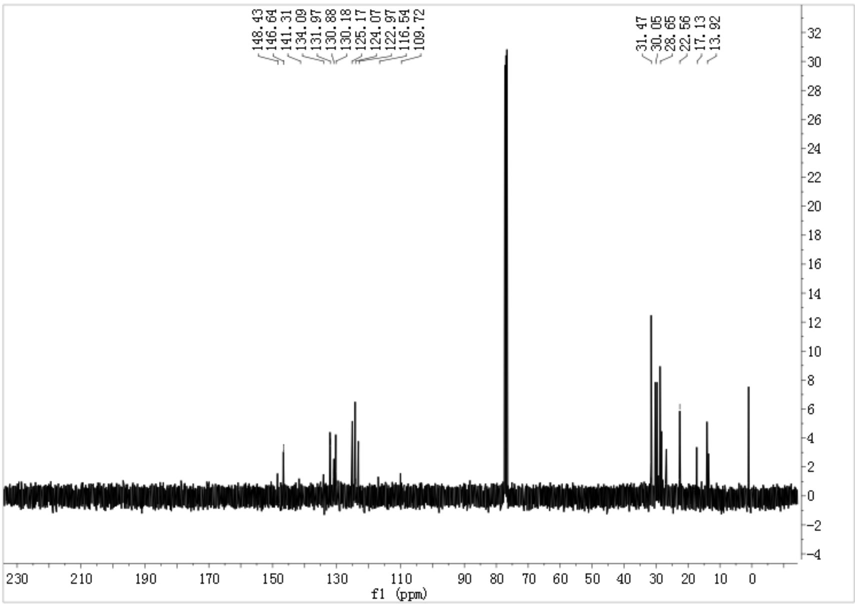

Figure S2. ^{13}C NMR spectra of compound **4** in $CDCl_3$.

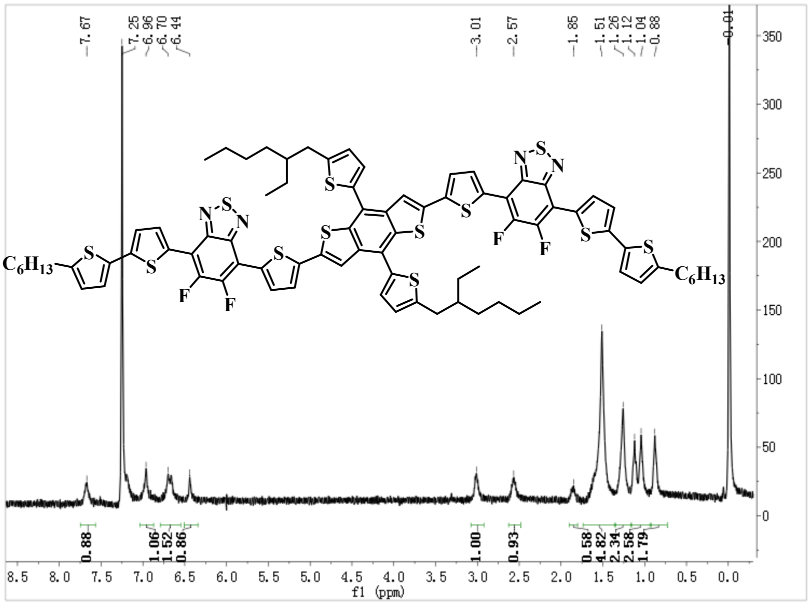

Figure S3. ^{1}H NMR spectra of compound **BDT(TffBTTT6)$_2$** in $CDCl_3$.

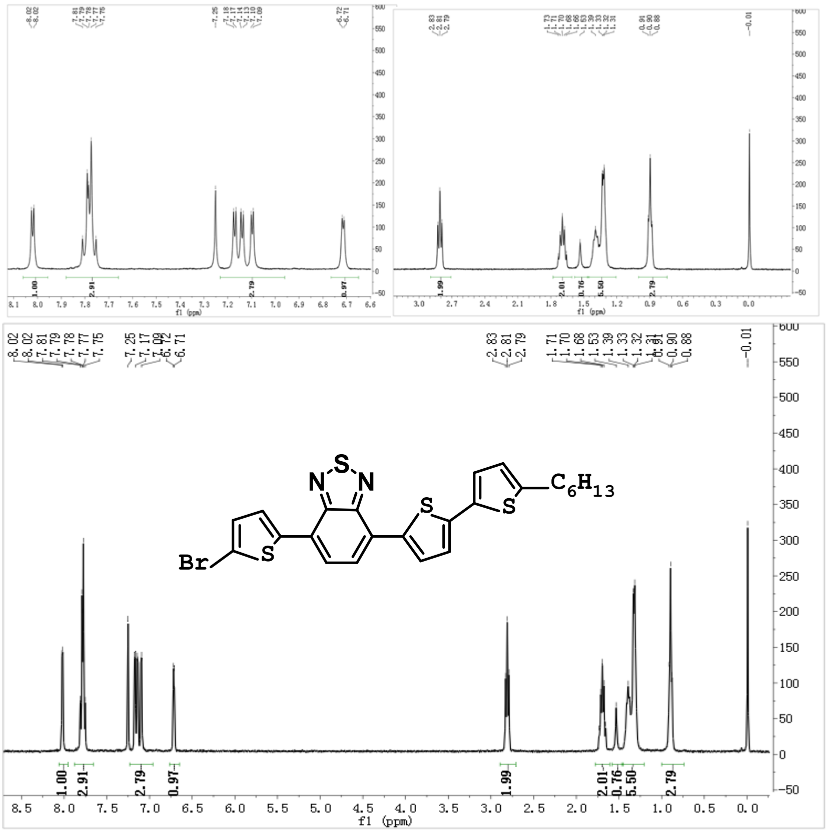

Figure S4. ^{1}H NMR spectra of compound **5** in $CDCl_3$.

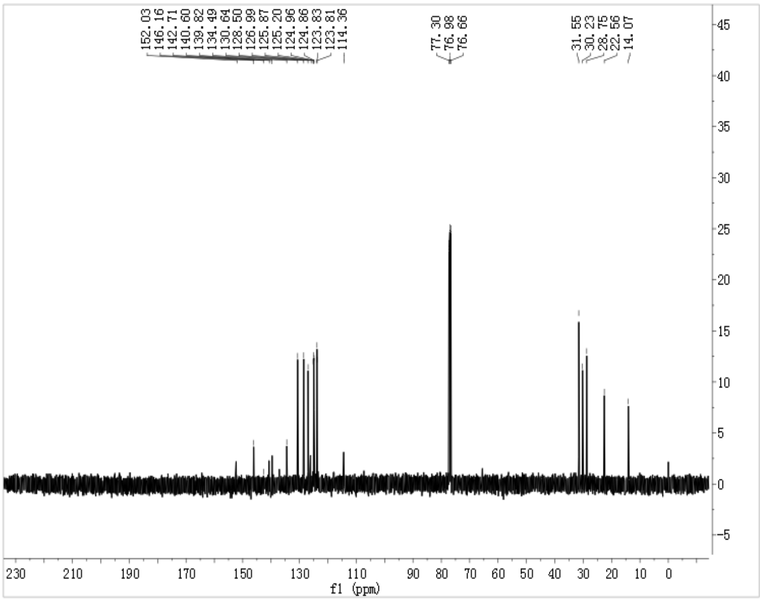

Figure S5. ^{13}C NMR spectra of compound **5** in $CDCl_3$.

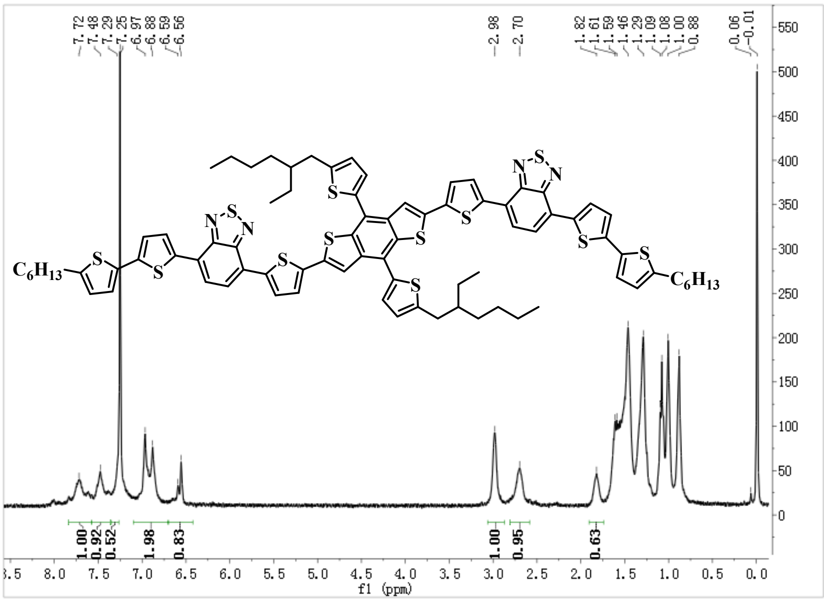

Figure S6. ^{1}H NMR spectra of compound **BDT(TBTTT6)$_2$** in $CDCl_3$.

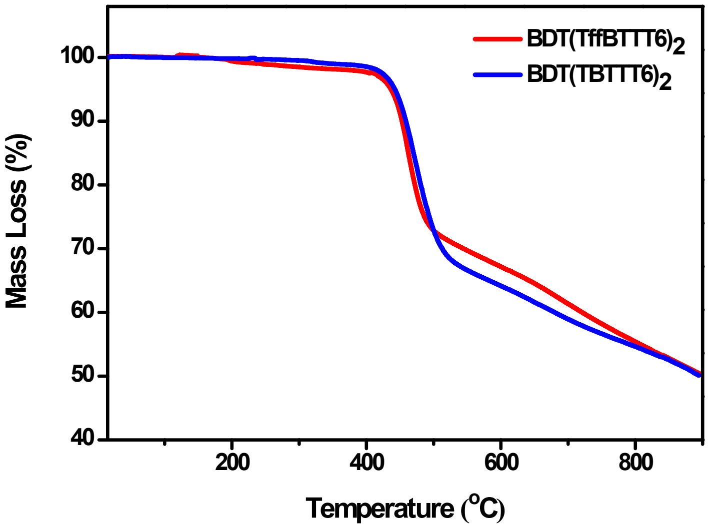

Figure S7. TGA plots of BDT(TffBTTT6)$_2$ and BDT(TBTTT6)$_2$ with a heating rate of 10 °C/min under N_2 atmosphere.

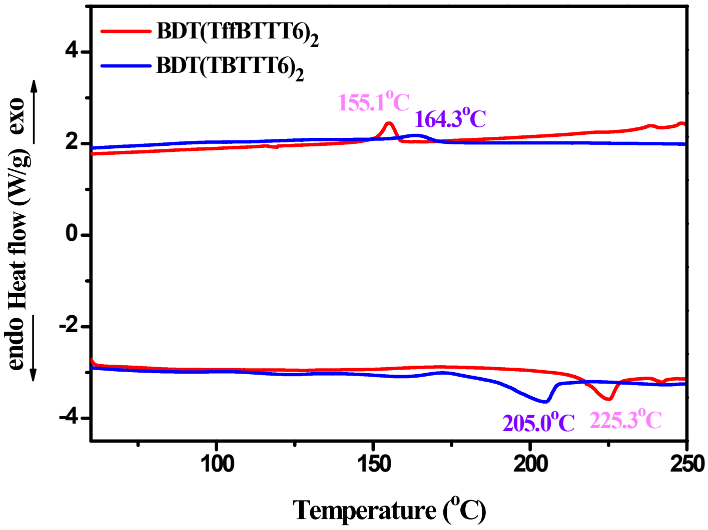

Figure S8. DSC thermograms of BDT(TffBTTT6)$_2$ and BDT(TBTTT6)$_2$ with a heating rate of 5 °C/min.

Table S1. Photovoltaic performance of BHJ solar cells based on BDT(TffBTTT6)$_2$/PC$_{71}$BM with different weight ratios (w:w) cast from CHCl$_3$ under illumination of AM 1.5 G, 100 mW cm^{-2} .

Ratio of donor and acceptor	V_{oc} (V)	J_{sc} (mA cm^{-2})	FF (%)	PCE (%)
1:1.5	0.71	1.84	61.1	0.8
1:1	0.72	1.56	57.8	0.7
1:0.8	0.73	2.97	59.8	1.3
1.5:1	0.73	2.83	58.5	1.2

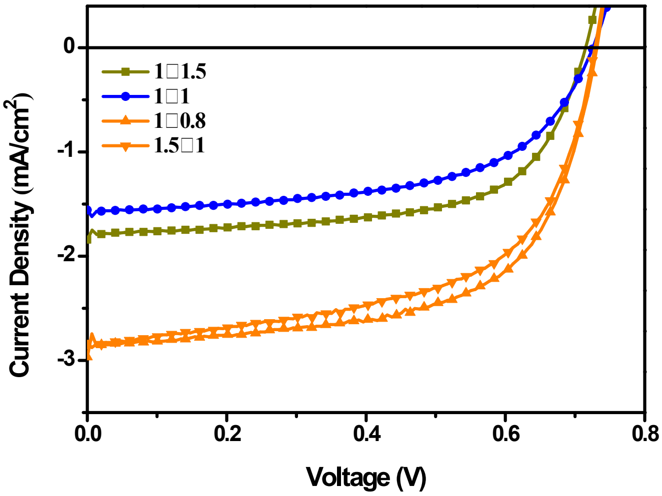

Figure S9. *J-V* curves of BHJ solar cells based on BDT(TffBTTT6)$_2$/PC$_{71}$BM with different weight ratios (w/w) cast from CHCl$_3$ under illumination of AM 1.5 G, 100 mW cm^{-2}.

Table S2. Photovoltaic performance of BHJ solar cells based on BDT(TffBTTT6)$_2$/PC$_{61}$BM and BDT(TBTTT6)$_2$/PC$_{71}$BM with weight ratio at 1:0.8 cast from CHCl$_3$ with thermal annealing at different temperature for 10 min under illumination of AM 1.5 G, 100 mW cm^{-2} .

active layer	Temperature (°C)	V_{oc} (V)	J_{sc} (mA cm^{-2})	FF (%)	PCE (%)
BDT(TffBTTT6)$_2$/	No	0.8	3.79	58.0	1.76
PC$_{61}$BM	70	0.82	4.09	59.5	2.0
	100	0.83	4.32	60.5	2.17
	160	0.80	5.77	56.1	2.59
BDT(TBTTT6)$_2$/	No	0.72	4.77	37.9	1.3
PC$_{71}$BM	70	0.67	6.19	37.0	1.53
	100	0.68	6.98	38.0	1.8
	170	0.79	3.13	34.7	0.86

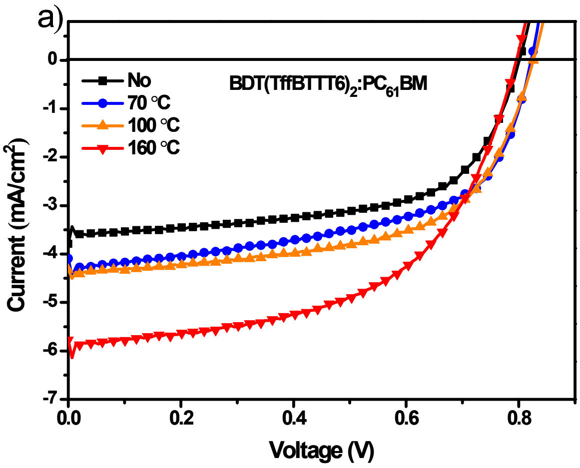

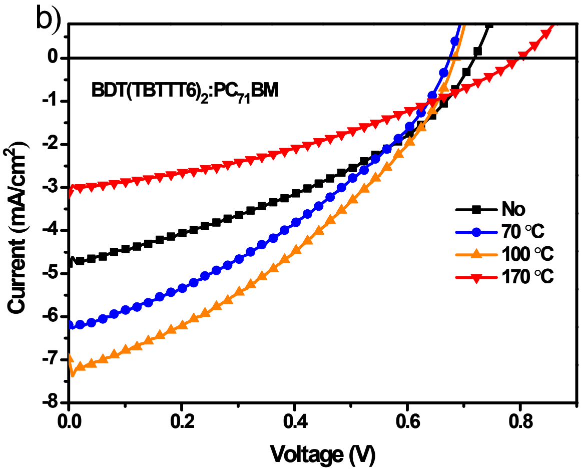

Figure S10. *J-V* curves of BHJ solar cells based on (a) BDT(TffBTTT6)$_2$/PC$_{61}$BM and (b) BDT(TBTTT6)$_2$/PC$_{71}$BM with weight ratio at 1:0.8 cast from CHCl$_3$ with thermal annealing at different temperature for 10 min under illumination of AM 1.5 G, 100 mW cm^{-2}.

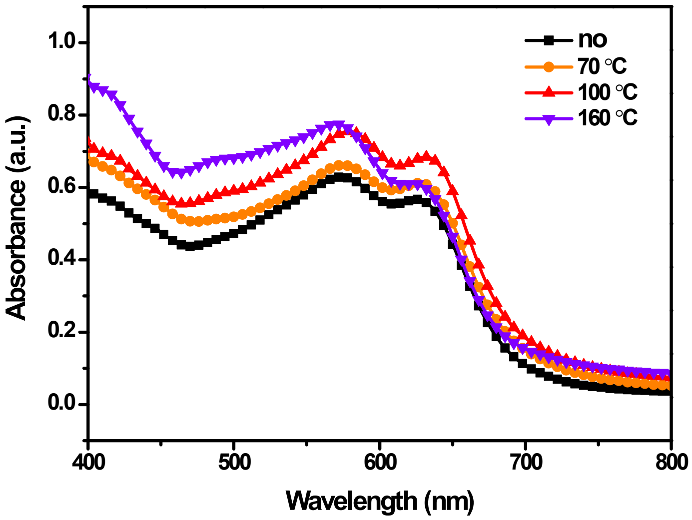

Figure S11. UV–vis absorption spectra of BDT(TffBTTT6)$_2$/PC$_{61}$BM blend film with thermal annealing for 10 min.

Table S3. Photovoltaic performance of BHJ solar cells based on BDT(TffBTTT6)$_2$/PC$_{61}$BM and BDT(TBTTT6)$_2$/PC$_{71}$BM with weight ratio at 1:0.8 cast from CHCl$_3$ with different volume ratios (v/v) of DIO under illumination of AM 1.5 G, 100 mW cm^{-2}.

active layer	DIO (%)	V_{oc} (V)	J_{sc} (mA cm^{-2})	FF (%)	PCE (%)
BDT(TffBTTT6)$_2$/	No	0.8	3.79	58.0	1.76
PC$_{61}$BM	0.5	0.73	6.86	62.2	3.11
	1.0	0.72	5.82	59.8	2.51
	2.0	0.68	5.53	46.1	1.73
BDT(TBTTT6)$_2$/	No	0.72	4.77	37.9	1.3
PC$_{71}$BM	0.5	0.71	7.90	50.3	2.82
	1.0	0.62	7.06	47.7	2.09
	2.0	0.61	5.53	39.2	1.32

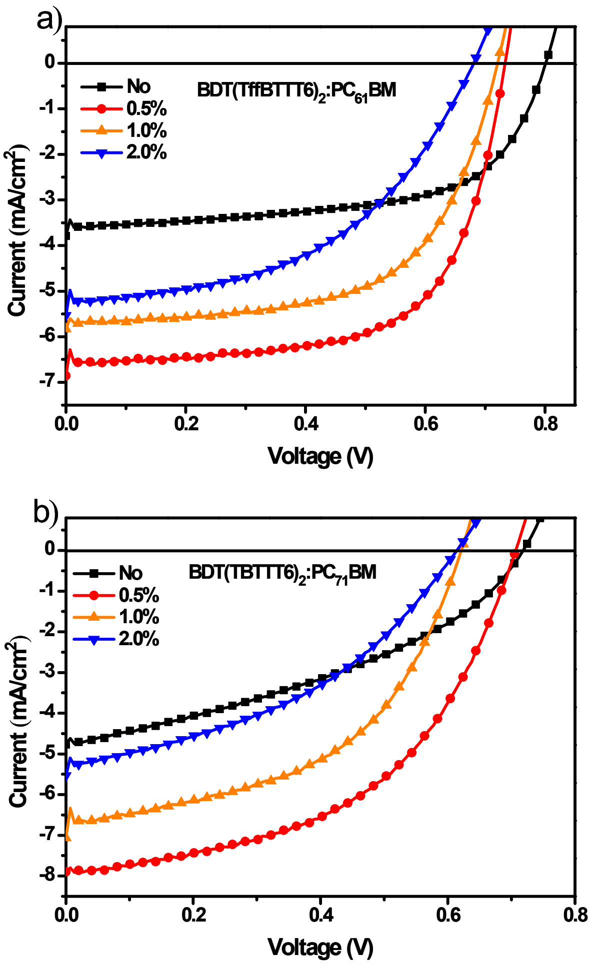

Figure S12. *J-V* curves of BHJ solar cells based on (a) BDT(TffBTTT6)$_2$/PC$_{61}$BM and (b) BDT(TBTTT6)$_2$/PC$_{71}$BM with weight ratio at 1:0.8 cast from CHCl$_3$ with different volume ratios (v/v) of DIO under illumination of AM 1.5 G, 100 mW cm^{-2}.

Table S4. Photovoltaic performance of BHJ solar cells based on BDT(TffBTTT6)$_2$/PC$_{61}$BM and

BDT(TBTTT6)$_2$/PC$_{71}$BM with weight ratio at 1:0.8 cast from CHCl$_3$ with 0.5 (v/v)% DIO and thermal annealing at different temperature for 10 min under illumination of AM 1.5 G, 100 mW cm^{-2}.

active layer	Temperature (°C)	V_{oc} (V)	J_{sc} (mA cm^{-2})	FF (%)	PCE (%)
BDT(TffBTTT6)$_2$/	No	0.73	6.86	62.2	3.11
PC$_{61}$BM	70	0.73	9.13	62.5	4.17
	100	0.67	7.16	56.3	2.7
	160	0.67	5.88	40.0	1.58
BDT(TBTTT6)$_2$/	No	0.71	7.90	50.3	2.82
PC$_{71}$BM	70	0.71	8.42	53.0	3.17
	100	0.64	6.22	49.5	1.97
	170	0.59	3.69	35.5	0.77

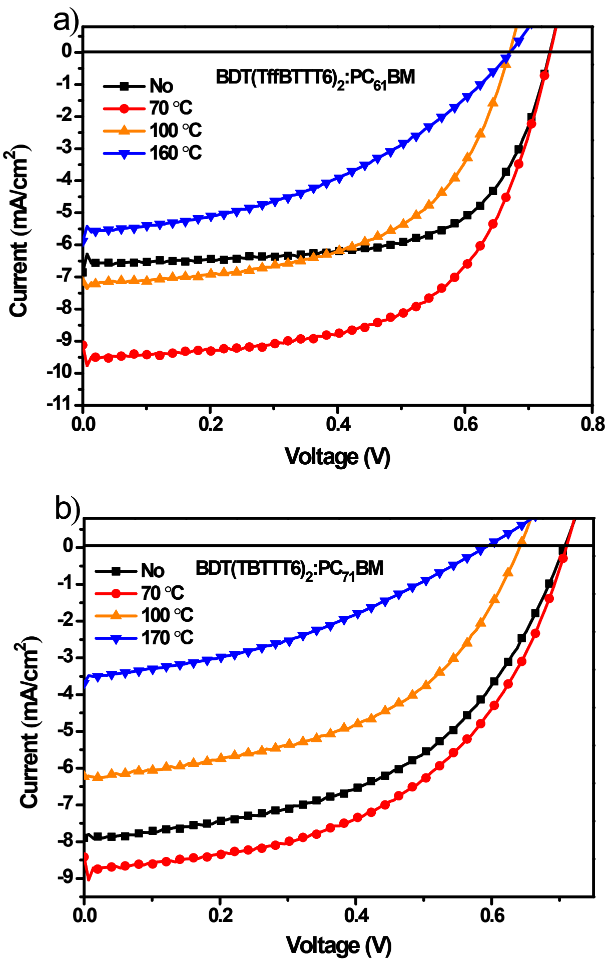

Figure S13. *J-V* curves of BHJ solar cells based on (a) BDT(TffBTTT6)$_2$/PC$_{61}$BM and (b) BDT(TBTTT6)$_2$/PC$_{71}$BM with weight ratio at 1:0.8 cast from CHCl$_3$ with 0.5 (v/v)% DIO and thermal annealing at different temperature for 10 min under illumination of AM 1.5 G, 100 mW cm^{-2}.

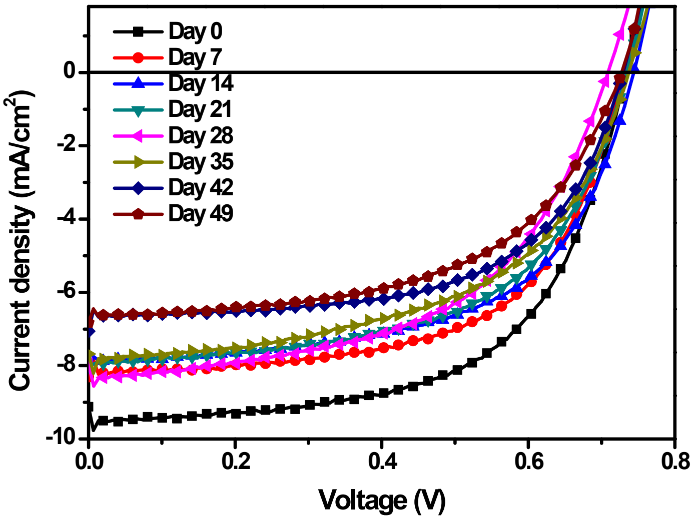

Figure S14. The *J*–*V* characteristics of this long-term stable device as a function of time for the devices: ITO/ZnO/BDT(TffBTTT6)$_2$:PC$_{61}$BM /MoO$_3$/Ag at glovebox.

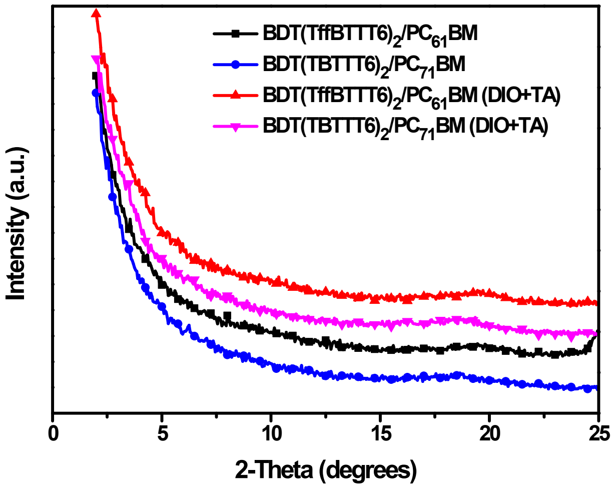

Figure S15. in-plane grazing incident X-ray diffraction (GIXRD) measurement of BDT(TffBTTT6)$_2$/PC$_{61}$BM and BDT(TBTTT6)$_2$/PC$_{71}$BM film with or without 0.5 v/v% DIO and 70 °C annealing (TA).

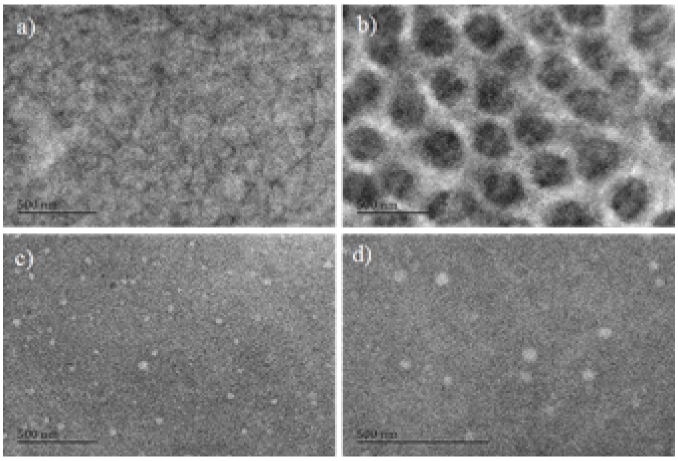

Figure S16. TEM images of the active layers with (a) BDT(TffBTTT6)$_2$/PC$_{61}$BM, (b) BDT(TffBTTT6)$_2$:PC$_{71}$BM, (c) BDT(TBTTT6)$_2$/PC$_{61}$BM, (d) BDT(TBTTT6)$_2$/PC$_{71}$BM.

References

1 H. C. Chen, C. W. Lai, I. C. Wu, H. R. Pan, I. Chen, P. Wen, Y. K. Peng, C. L. Liu, C. h. Chen, P. T. Chou, *Adv. Mater.* **2011,** *23*, 5451-5455.

2 Y. J. Cheng, C. H. Hsieh, P. J. Li, C. S. Hsu, *Adv. Funct. Mater.* **2011,** *21*, 1723-1732.

3 Y. Liu, X. Wan, F. Wang, J. Zhou, G. Long, J. Tian, Y. Chen, *Adv. Mater.* **2011,** *23*, 5387-5391.